(2001) Computational Modeling in Biological Fluid Dynamics
L.J. Fauci & S. Gueron [Eds]. New York: Springer Verlag

FLUID DYNAMICS OF ANIMAL APPENDAGES THAT CAPTURE MOLECULES: ARTHROPOD OLFACTORY ANTENNAE

M.A.R. KOEHL*

1. Introduction. Appendages bearing arrays of hair-like structures serve important biological functions in many animals from a variety of phyla. For example, feathery gills take up oxygen, hairy olfactory antennae capture odorant molecules, filamentous suspension-feeding structures catch single-celled algae, setulose appendages create ventilatory or feeding currents, and bristly legs or wings propel little animals through the surrounding water or air. To perform any of these functions, an array of hairs must interact with the fluid around it. Therefore, in order to elucidate basic rules governing how hairy appendages work, we have been studying the fluid dynamics of arrays of cylinders. The purpose of this paper is to provide a brief overview of what mathematical and physical models have taught us about fluid motion around and through arrays of hairs, and of how those insights have helped us unravel ways in which the function of hairy appendages depends on their structure and behavior. I will focus on examples of appendages that capture molecules: the olfactory antennae of various arthropods.

2. Fluid flow near hairs in an array.

Overview. The Reynolds numbers of the hairs on the types of appendages listed above are generally of order 10^{-5} to 10 (reviewed in Rubenstein and Koehl, 1977; LaBarbera, 1984; Cheer and Koehl, 1987a; Shimeta and Jumars, 1991; Loudon, et al., 1994). Reynolds number (Re= UL/ν, where U is velocity, L is a linear dimension, in this case hair diameter, and ν is the kinematic viscosity of the fluid) represents the ratio of inertial to viscous forces for a particular flow situation. At the low and intermediate Re's at which these hairs operate, viscosity is very important in determining flow patterns, although inertia cannot be ignored for hairs operating at the upper end of this Re range. When a hair moves through a viscous fluid, the layer of fluid in contact with its surface does not slip relative to the surface and a velocity gradient develops in the fluid around the hair. The lower the Re, the thicker this layer of sheared fluid is relative to the dimensions of the hair. If the layers of fluid moving along with the hairs in an array are thick relative to the gaps between the hairs, then little fluid may leak through the array.

We have defined the "leakiness" of a gap between neighboring hairs in an array as the ratio of the volume of fluid that flows through the gap in a

*Department of Integrative Biology, University of California, Berkeley, CA 94720-3140, U.S.A.

(The IMA Volumes in Mathematics and its Applications)

unit of time to the volume of fluid that would have flowed (at freestream velocity) through a space of that width if there were no hairs present (Cheer and Koehl, 1987a). A hair-bearing appendage with a high leakiness functions like a sieve. In contrast, fluid moves around rather than through an array of hairs with low leakiness, hence an appendage bearing such an array is functionally a paddle even though it is full of holes.

If we consider appendages like olfactory antennae or gills that capture molecules on hair-like structures, the volume of fluid that can be filtered per time depends on the leakiness of the array of hairs on the appendage. Furthermore, the steepness of the velocity gradients near individual hairs affects the flux of molecules to the surfaces of the hairs (e.g. Adam and Delbruck, 1968; Berg and Purcell, 1977; Murray, 1977; Schmidt and Ache, 1979; Futrelle, 1984; Atema, 1985; Moore, et al., 1991; Koehl, 1996).

Approaches to Studying Flow Through Hairy Appendages. Fluid movement around and through arrays of hairs can be studied using various empirical and theoretical tools. Although technically challenging, we can measure the kinematics of hair-bearing appendages on real organisms as well as the fluid velocities around them (e.g. Koehl and Strickler, 1981; Koehl, 1993; 1995; Mead, et al., 1999). However, the details of velocity profiles around individual microscopic hairs on rapidly-moving appendages are difficult to resolve. Another limitation of working with living organisms is that the range of morphologies and behaviors available in nature limits our ability to quantify the consequences of particular aspects of structure or motion; when using real organisms, it is usually not possible to systematically vary only one parameter at a time while holding all others constant to quantify the effects of each.

In contrast, mathematical and physical models permit us to study combinations of morphology and behavior not found in nature, thereby enabling us to tease out the roles played by specific aspects of structure or motion and to quantify the effects on performance of changes in defined parameters. Mathematical and physical models also enable us to quantify aspects of the behavior of a system that are difficult to measure on living organisms, such as velocity gradients around individual microscopic hairs on a flapping appendage.

Repeatable velocity and force measurements with fine spatial and temporal resolution that cannot be made on uncooperative, delicate microscopic organisms are technically possible with large physical models if they are scaled properly. If a model and a real appendage are geometrically similar and operate at the same Re, they are dynamically similar (i.e. the ratios of velocities and forces at analogous points in the fluid around the model and the appendage are the same). Therefore, a large model moved at a conveniently slow speed in a Newtonian viscous syrup can be used to study the fluid dynamics of a microscopic appendage operating at the same Re in water or air.

3. Models of fluid motion between cylinders.

Mathematical Models of Filters and Porous Screens. Various methods have been used to calculate fluid motion through filters composed of arrays of fibers (reviewed in e.g. Fuchs, 1964; Davies, 1973; Laws and Livesey, 1978). For example, Tamada and Fujikawa (1957) modeled the two-dimensional flow at low Re through an infinite row of cylinders. All the fluid must flow through the gaps between hairs in an infinite array, therefore such models are not appropriate for predicting the flow between hairs on appendages of finite width because fluid can flow around as well as through such appendages. Mesh-like structures of finite width have been modeled as porous plates, and a variety of methods for calculating the flow through and around them have been used (e.g. Taylor and Batchelor, 1949; Spielman and Goren, 1968; and Koo and James, 1973). One approach that has been used to estimate the flow through biological filters is a modification of Tamada and Fujikawa's model (Silvester, 1983) .The predictions of Silvester's model agree reasonably well with water flow measured through the silk feeding nets spun by aquatic caddisfly larvae (Loudon, 1990), but underestimate flow through feathery moth antennae and through bristly filter-feeding fans of aquatic black fly larvae (Cheer and Koehl, 1987b). Flow through biological filters has also been estimated using Darcy's law (Cheer and Koehl, 1987b), which yields leakiness values for various insect filters that are orders of magnitude too low when compared with empirical data (Cheer and Koehl, 1987b). These comparisons of model results with biological data suggest that porous plate models are only appropriate for arrays of hairs that form screens, such as caddis fly nets or appendages with hairs bearing bristles that completely span the gaps between adjacent hairs. In contrast, the modeling approach of Cheer and Koehl (1987a; 1987b) yields much better matches with empirical measurements of flow through hairy appendages.

Mathematical Model of Flow Between a Pair of Cylinders. Cheer and Koehl (1987a) calculated fluid movement between and around a pair of circular cylinders at low Re using a two-dimensional model. Fluid velocities near the cylinders were calculated in bipolar coordinates using Stoke's low-Reynolds-number approximation of the Navier-Stokes equation, and fluid velocities far from the cylinders were calculated in polar coordinates using Oseen's low-Re approximation, which includes inertial effects. These flow fields were combined using a matched asymptotic expansion technique, and the velocity profiles predicted by this model were used to determine the leakiness of pairs of hairs operating at a variety of biologically-relevant Re's and spacings (described by the ratio of the width of the gap between neighboring hairs to the diameter of a hair (G/D)).

The calculations of Cheer and Koehl (1987a) reveal that a transition in the function of an array of hairs, between operating like a solid paddle and functioning like a leaky sieve, occurs as Re is changed between 10^{-2} and 1. The leakiness of a pair of hairs depends not only on Re, but also

on the spacing (G/D) of the hairs. At very low Re (Re $\leq 10^{-3}$), little fluid moves through the gap between adjacent hairs (even when G/D is high), thus appendages whose hairs operate at such low Re's should behave like paddles. In contrast, at Re near 1, little fluid is dragged along with cylinders as they move, and hairy appendages should be sieve-like unless G/D is very low (Fig. 1). The more-closely-spaced the hairs (i.e. the lower the G/D), the higher the Re at which the transition to being leaky occurs. The model of Cheer and Koehl predicts that, at Re's of order 10^{-1} to 1, the leakiness of appendages with closely-spaced hairs is very sensitive to changes in velocity or changes in G/D (Fig. 1).

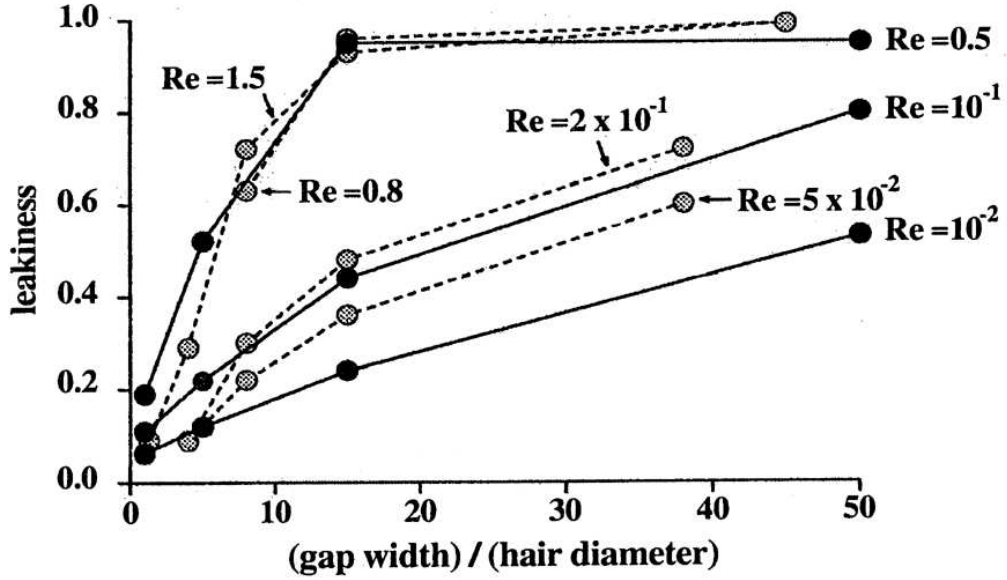

FIG. 1. *Leakiness (the ratio of the volume of fluid that flows in a unit of time through the gap between neighboring hairs to the volume of fluid that would have flowed at freestream velocity through a space of that width if there were no hairs present) plotted as a function of G/D, the ratio of the width of the gap between adjacent hairs to the diameter of a hair. Black circles connected by solid lines indicate leakiness values calculated using the model of Cheer and Koehl (1987a). Grey circles connected by dashed lines represent leakiness measured during towing experiments with comb-like physical models (Hansen and Tiselius, 1982). Reynolds number (Re) for each line was calculated using hair diameter for the linear dimension.*

The model of Cheer and Koehl can be used to estimate the flow through feathery appendages composed of hairs that bear bristles (Cheer and Koehl, 1987b). First the velocity profile between neighboring hairs is calculated; this velocity profile is then used to determine the freestream velocity encountered at defined positions along the length of a bristle, and the velocity profile between adjacent bristles is then calculated. Leakiness calculated using this approach provides a good match with measured values for a variety of feathery appendages of insects and crustaceans (Cheer and Koehl, 1987b; Koehl, 1993; 1995).

Physical and Numerical Models of Flow Through Rows of Hairs. The model described in Cheer and Koehl (1987a) only deals with two cylinders at Re < 1, whereas most hairy appendages bear more than two hairs and some animals operate their hairs at Re > 1. Hansen and Tiselius (1992) measured flow through physical models bearing a comb-like row of cylinders that were towed through mixtures of glycerol and water to yield a range of Re's. Their leakiness results are similar to those calculated by Cheer and Koehl (1987a) (Fig. 1). Abdullah and Cheer (unpublished; described in Koehl, 1993) used a numerical model to compute the steady, two-dimensional flow near cylinders at Re's between 0.5 and 4 to investigate the consequences of adding more cylinders to a row. Their model predicts that the addition of more hairs to a row reduces leakiness if Re $<$ 1, but increases leakiness if Re > 1; measurements of flow through physical models have shown the same phenomenon (reviewed in Koehl, 1995).

Leonard (1992) and Hansen and Tiselius (1992) measured flow through comb-like physical models at Re's up to 40, higher than those at which the mathematical model of Cheer and Koehl (1987a) is applicable. These physical models revealed that leakiness is very sensitive to hair spacing only when hairs are very close together at Re's of order 10, and that the critical G/D below which gap width affects leakiness becomes lower as Re is increased (Koehl, 1995).

Hair-bearing appendages generally operate near solid boundaries (such as the body surface of an animal, the wall of a burrow, or the substratum in an animal's habitat). Loudon, et al. (1994) measured the leakiness of pairs of cylinders towed along or towards a wall. We found that, at Re's of 10^{-2} and lower, leakiness was increased by movement near a wall. In contrast, we found that leakiness of models towed near a wall at Re's of 10^{-1} and 1 matched the theoretical values for cylinders in an unbounded fluid. This suggests that a behavior that is effective at altering leakiness at very low Re (i.e. moving close to the body surface or another wall) does not change leakiness at intermediate Re.

The mathematical model of Cheer and Koehl (1987a; 1987b) is two-dimensional, thus it does not address the consequences of fluid flowing around the tips of hairs of finite length. Our experiments with physical models indicated that the leakiness of the gap between cylinders operating at Re's $\leq 10^{-2}$ is lower for cylinders of finite length than for those infinitely long because fluid is free to flow around the tips of the appendage as well as around the sides (Koehl, 1995). The physical models of Hansen and Tiselius (1992) showed that increasing hair length-to-diameter ratio can decrease comb leakiness at Re $\geq 10^{-2}$.

Summary. Both mathematical and physical models of rows of cylinders show that a transition in the leakiness of an array of hairs occurs at low or intermediate Re. Furthermore, mathematical and physical models of hair-bearing appendages of particular species of animals also show a transition between non-leaky paddle-like behavior and leaky sieve-like

function if speed is increased in this Re range (Koehl, 1995; 1998). These various models predict that the finer the mesh (i.e. the lower the G/D) of the appendage, the higher the Re at which this transition between paddle-like and sieve-like function occurs. The models also predict that, at Re's of order 1, leakiness is very sensitive to hair spacing and to flow velocity if the G/D of the hairs is small. Armed with the insights that models of flow between cylinders have provided about how morphology and behavior affect the leakiness of hair-bearing appendages, let us now consider the molecule-capturing performance of hairy olfactory antennae of different designs.

4. Olfactory antennae.

Background. Many animals use chemical cues in the water or air around them while performing ecologically-important activities such as locating food, selecting habitats, detecting predators or competitors, and communicating with conspecifics (e.g. reviewed in Cardé, 1984; Atema, 1985; 1995; Zimmer-Faust, 1989; Murlis, et al., 1992; Koehl, 1996). The arrival of odorant molecules from the environment to the surface of a chemosensory structure is a critical step in the process of olfaction. From a fluid dynamic standpoint, this process can be broken into two regimes based on scale: 1) large-scale turbulent flow of water or air transports the odorant from the source to the immediate vicinity of the sensor; and 2) small-scale viscous flow and molecular diffusion transport the odorant to the surface of the sensor (e.g. DeSimone 1981; Koehl 1996). The first step in filtering the spatial and temporal information contained in an odor plume (e.g. Murlis, 1986; Weissburg and Zimmer-Faust, 1994; Willis, et al., 1994; Atema, 1995) is therefore due to the physical manner in which an olfactory structure affects fluid flow across its surfaces (e.g. Moore, et al., 1989; Atema, 1995; Koehl, 1996).

The olfactory antennae of many organisms are appendages bearing arrays of microscopic hairs containing chemosensory neurons (e.g. Zacharuk, 1985; Halberg, et al., 1992); such antennae pick up chemical signals from the surrounding fluid, water or air. Water or air moves relative to an olfactory antenna as an animal locomotes, experiences ambient currents or wind, creates flow past itself, or flicks the antenna. The Re's of the olfactory hairs on a variety of arthropods range from $\leq 10^{-4}$ to 10 (Loudon, et al., 1994). In this Re range, the viscous flow near sensory hairs is laminar. Therefore, molecular diffusion is the mechanism that moves odorants across streamlines towards or away from the surface of a chemosensory hair.

Some researchers have argued that the diffusion of molecules to olfactory receptors determines the temporal pattern of the onset of neural responses to odorants (e.g. Getchell & Getchell 1977; DeSimone 1981; Nachbar & Morton 1981; Moore et al. 1989), whereas others have suggested that molecular diffusion does not limit the access of odor molecules to receptors (Futrelle 1984; Mankin and Mayer 1984; Boeckh, et al. 1965).

Calculations of odorant interception by a chemosensory hair modeled as an isolated, infinitely-long cylinder indicated that increasing the flow velocity encountered by the hair has a relatively small effect on the rate of chemical signal interception by the hair (Adam and Delbruck, 1968; Murray, 1977). In contrast, increasing the fluid velocity encountered by a chemosensory antenna made up of an array of cylinders (rather than a single cylinder) may have a large effect on chemical signal interception by a sensory hair in that array *if* the velocity increase occurs in the Re range in which the leakiness of that array of hairs is sensitive to velocity (Koehl, 1996).

In spite of the importance of small-scale fluid flow to molecule capture, information has been lacking about velocity profiles near chemosensory hairs on real olfactory appendages.

5. Leakiness of arrays of hairs on olfactory appendages.

Olfactory Antennules of Crustaceans. Many malacostracan crustaceans, such as lobsters, stomatopods ("mantis shrimp"), and crabs, capture odorant molecules with appendages called antennules (Fig. 2A, C, E). The lateral branch of such an antennule bears chemosensory hairs called "aesthetascs" (Heimann, 1984; Laverack, 1988) that serve an olfactory function (evidence reviewed by e.g. Atema, 1977; 1995; Gleeson, 1982; Grunert and Ache, 1988; Hallberg, et al. 1992; Atema and Voigt, 1995). Lateral branches of crustacean antennules are often used as model systems for studying the electrophysiology of olfactory neurons (reviewed by e.g. Ache, 1982; 1988; Atema, 1985; Marscall and Ache, 1989; Michel, et al., 1991; Atema and Voigt, 1995). Aesthetasc arrangement varies between species. For example, the aesthetascs on the antennules of a spiny lobster are arranged in complex, zig-zag rows surrounded by a cage of larger non-sensory guard hairs (Fig. 2B), the aesthetascs on the antennules of a stomatopod are arranged in simple, sparse rows (Fig. 2D), and the aesthetascs on the antennules of a crab are arranged in a densely-packed tuft resembling a toothbrush (Fig. 2F). We have used a combination of experiments and mathematical models to investigate the functional consequences of these different antennule designs.

A variety of crustaceans, such as lobsters, stomatopods, and crabs, flick their olfactory antennules through the surrounding water. It has been suggested that antennule flicking is a mechanism of increasing water penetration into an array of aesthetascs, thereby enhancing the access of odors to receptor cells (e.g. Snow, 1973; Schmidt and Ache, 1979; Atema, 1985; Gleeson, et al., 1993). Several lines of evidence are consistent with this idea. Pulses of flowing water (to mimic flicking) onto the aesthetascs of antennule preparations increased penetration of tracer molecules into the water between aesthetascs (Moore, et al., 1989; 1991) and enhanced the response of lobster olfactory receptor neurons to changes in odor concentration (Schmidt and Ache, 1979).

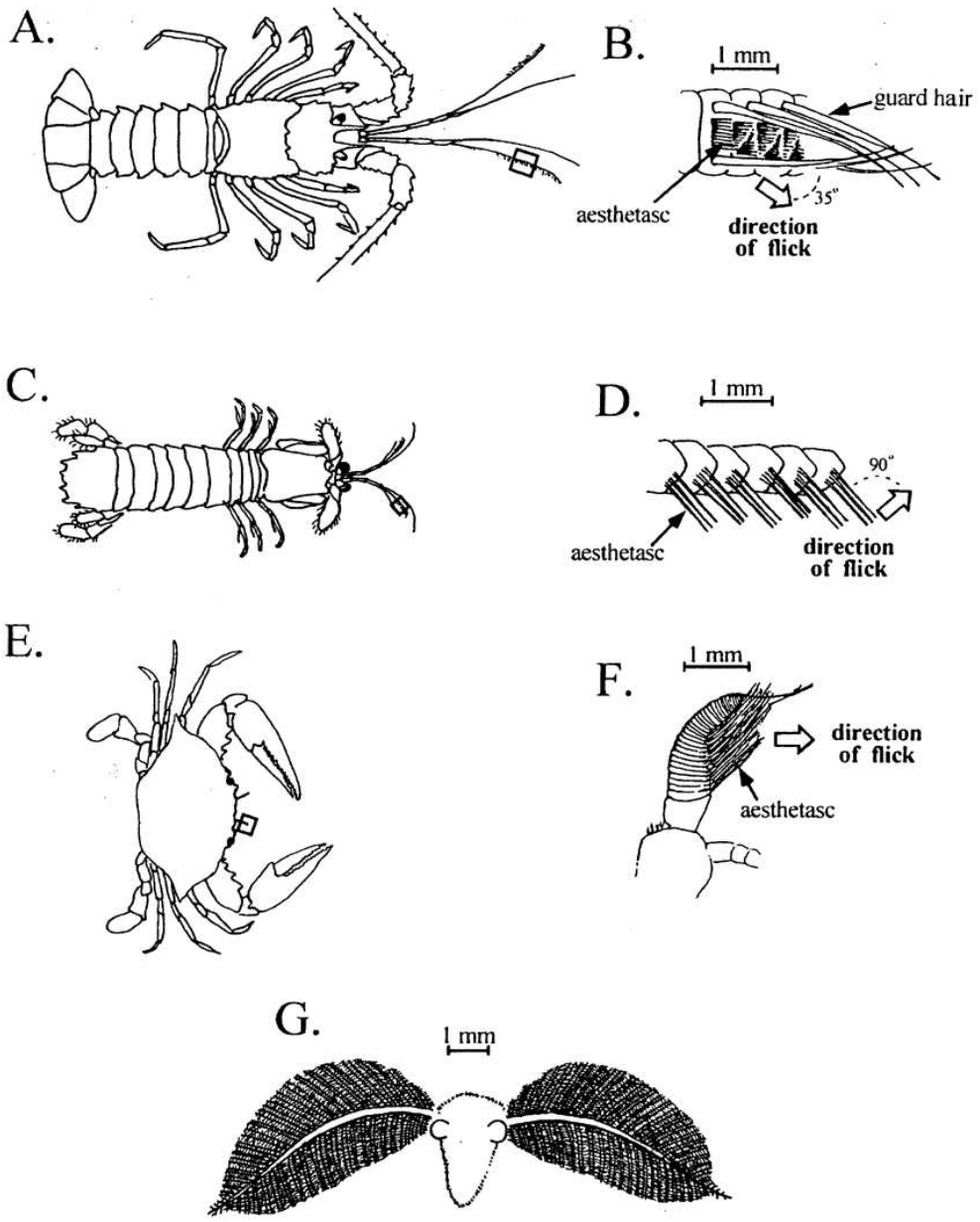

FIG. 2. *Examples of arthropods with hair-bearing olfactory appendages. The boxes around antennules in A, C, and E indicate the region of the antennule diagrammed in B, D, and F, respectively. A. Spiny lobster, Panulirus argus. B. Magnified view of a section of the lateral filament of a P. argus antennule. The lateral filament flicks downward, with the aesthetascs at an angle of ~35° to the direction of motion (Gleeson, et al., 1993). C. Stomatopod ("mantis shrimp" Squilla empusa. D. Magnified view of a section of the aesthetasc-bearing filament of a stomatopod antennule, Gonodactylus mutatus. The antennule flicks laterally, with the aesthetascs perpendicular to the direction of movement (Mead, et al., 1999). E. Blue crab, Callinectes sapidus. F. Magnified view of the tip of the antennule of a C. sapidus. The antennule can flick in many directions, but the aesthetascs point in the direction of motion during a flick (Martinez, Lee, and Koehl, unpublished data). G. Head of a male silkworm moth, Bombyx mori, showing the olfactory antennae. When the male fans his wings, air moves from front to back across the antennae (Loudon and Koehl, in press).*

Lobster antennules. We conducted a high-speed video analysis of the kinematics of flicking by the antennules of spiny lobsters, *Panulirus argus*, and a morphometric analysis of the hairs on the lateral branches of these antennules (Goldman and Koehl, submitted) (Fig. 2A, B). We found that during the rapid flick downstroke, the Re of the aesthetascs was 2, whereas during the slower upstroke, the Re was only 0.5. *P. argus* aesthetascs are closely packed ($G/D < 1$), hence we might expect a transition between leaky behavior during the downstroke and non-leaky behavior during the upstroke.

We tested this prediction by measuring the flow around a dynamically-scaled physical model of the lateral branch of a *P. argus* antennule (Koehl and Hu, unpublished data). The model was towed through a tank of viscous sugar syrup (technical details described in Loudon, et al., 1994) at the same orientation and Re used by *P. argus* antennules during the flick downstrokes and upstrokes. A sheet of laser light illuminated one plane normal to the long axis of the antennule model, and video records of the motions of neutrally-buoyant marker particles in the fluid in that plane were digitized. Examples of tracings of particle paths around the model during the rapid flick downstroke and the slower recovery stroke are shown in Figure 3. Fluid clearly moves through the array of aesthetascs during the leaky downstroke, but flows around the array during the non-leaky upstroke. This transition in leakiness of the aesthetasc array results in a flushing of old water out of the aesthetasc array during the downstroke, and a retention of a new water sample within the array during the upstroke. Therefore, because *P. argus* antennules operate at this critical range of aesthetasc Re's in which leakiness is sensitive to speed, they are able to take discrete water samples to smell with each flick, akin to sniffing.

We found that the Reynolds number (Re), and thus the flow regime, of *P. argus* aesthetascs during flicking was maintained as body size changed (Goldman and Koehl, unpublished data). Although we only examined animals representing a 33% change in body length, our results are consistent with those of Best (1995), who found only a slight change in aesthetasc Re over a 20-fold range of body lengths for the clawed lobster, *Homarus americanus*. Such maintenance during lobster growth of aesthetasc Re in the critical range in which leakiness is sensitive to flicking speed, suggests that the ability to take discrete water samples (i.e. to sniff) is maintained during the ontogeny of these animals. It also suggests that taking discrete samples in space and time may be important to processing information about the distribution of odorants in the environment.

Stomatopod antennules. Stomatopods ("mantis shrimp") have antennules bearing simple rows of aesthetascs (Fig. 2C, D). We conducted a high-speed video analysis of antennule flicking by stomatopods, *Gonodactylus metatus*, and a morphometric analysis of their aesthetascs; we examined animals representing a ten-fold range of body lengths, from small juveniles to adults (Mead, et al. 1999). We found that *G. mutatus* flick their anten-

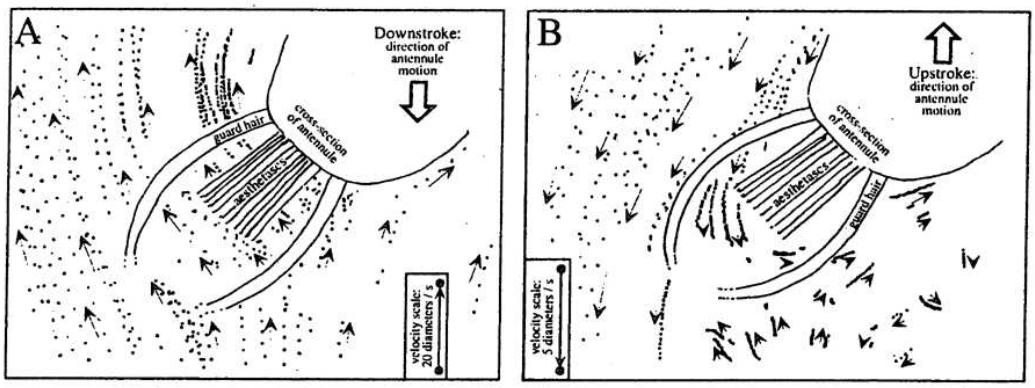

FIG. 3. *Diagrams of the fluid flow near a dynamically-scaled physical model of the lateral filament of the antennule of a spiny lobster, Panulirus argus, during the rapid flick downstroke (A) and the slower upstroke (B). The antennule filament is seen in cross-section, and the direction of antennule motion is indicated by the large arrow. One plane in the fluid was illuminated by a sheet of laser light. A video camera moving with the model recorded the motions relative to the model of neutrally-buoyant marker particles in the fluid (small arrows indicate the directions of fluid motion relative to the model). The dots on the diagrams indicate the positions of marker particles after successive time intervals; the closer the dots in a row within one diagram, the slower the flow at that position in the flow field. The velocity scale (shown in a box in each diagram) indicates the distance between particle positions in one time interval if the particle were moving 20 mm/s (A) or 5 mm/s (B). (Koehl and Hu, unpublished data).*

nules laterally, moving more rapidly during the outstroke than during the return stroke. Unlike lobsters, however, these stomatopods do not maintain the Re of their aesthetascs as they grow: the aesthetascs of small juveniles operate at Re's of order 10^{-1}, whereas those of adults operate at Re's of order 1. However, the G/D for aesthetascs in adjacent rows is much greater for juveniles than for adults.

We measured the flow around dynamically-scaled physical models of adult and juvenile *G. mutatus* antennules (Mead and Koehl, in press), using the techniques described above for lobster models. Our measurements of the leakiness of the aesthetasc arrays on these models when operating at a variety of different aesthetasc Re's showed that the adults and juveniles each operate at the Re's that maximize the ratio of leakiness during the outstroke to leakiness during the return stroke. The Re range that maximizes the ability of the antennule to take discrete water samples is lower for juveniles than for adults because juveniles have larger G/D's than do adults. Thus, like lobsters, stomatopods appear to maintain the ability to sniff during their ontogeny.

Crab Antennules. Brachyuran crabs, such as the blue crab *Callinectes sapidus*, flick small antennules bearing dense arrays of hairs (Fig. 2E, F). Our morphometric analysis of *C. sapidus* antennules and our high-speed video study of their flicking revealed that the aesthetascs operate at Re's of order 1 (Martinez, Lee, and Koehl, unpublished data). Videomicrog-

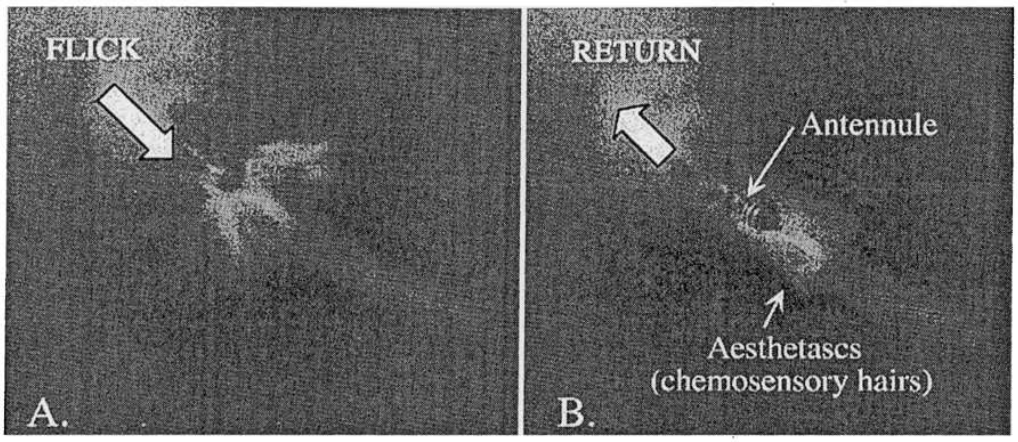

FIG. 4. *Frames of a video of an end-on view of the antennule of a blue crab, Callinectes sapidus, when exposed to flow that simulates the water motion relative to the antennule during the flick (A) and during the return stroke (B). The aesthetascs are passively splayed apart by the flow relative to the antennule during the flick (A), and are pushed together during the return stroke (B) (Koehl and Martinez, unpublished data).*

raphy of antennules exposed to water currents simulating the flow they experience during flicking revealed that the aesthetascs are flexible and are splayed apart during the flick downstroke, but are pushed together during the return stroke (Fig. 4). Because the aesthetascs operate at a Re range in which changes in the gap width between closely-spaced hairs can produce very large changes in leakiness (Cheer and Koehl, 1987; Koehl, 1995; 1996) (see Fig. 1), such aesthetasc splaying could lead to a substantial increase in flow between the hairs during the flick downstroke. We are currently using dynamically-scaled physical models to test this prediction.

Moth Antennae. Moths have feathery olfactory antennae (Fig. 2G) composed of chemosensory hairs (sensilla) borne on rows on larger branches. Previous models of molecule interception by a moth sensillum have assumed a single infinitely-long hair (Adam and Delbruck, 1968; Murray, 1977), although Murray (1977) pointed out that the flow near a sensillum surrounded by others would be slower than around an isolated cylinder. Indeed, measurements (Vogel, 1983) and mathematical modeling (Cheer and Koehl, 1987b) of the airflow through the feathery antennae of male *Acitas luna* moths indicate that the leakiness of these olfactory structures is only ~0.08 at air velocities they would encounter on a flying moth.

We have used a combination of experiments and mathematical modeling to study the airflow through the olfactory antennae of male silkworm moths, *Bombyx mori* (Loudon and Koehl, unpublished data). Most of the sensory hairs on the antennae of *B. mori* adult males are sensitive to a specific molecule, the sex pheromone emitted by conspecific females (e.g.

Gnatzy, et al. 1984; Steinbrecht 1992; Pophof, 1997). Silkworm moths do not fly, but males fan their wings when exposed to the female pheromone. We have used hot-film anemometry to measure the air velocities encountered by the antennae on fanning male moths, and have used these data to estimate (employing the approach of Cheer and Koehl, 1987b) the velocity profiles between the sensilla. We found that the difference between air penetration through an antenna on a moth fanning his wings versus on a moth walking without fanning is impressive: wing fanning produces air flow that is 15 times faster than that generated by walking at top speed, but the air velocities this produces through the gaps between sensilla is predicted to be ~560 times faster. This enormous increase in flow between sensilla occurs because the velocity at which moths fan is fast enough to produce a transition to leaky behavior for the array of closely-spaced hairs on their antennae.

Summary. The diverse examples of olfactory antennules and antennae described above appear to operate in a range of hair spacings (G/D) and Re's at which changes in velocity or in G/D can have a big effect on leakiness. Therefore, by altering the fluid velocity encountered by an olfactory appendage (via flicking in lobsters, stomatopods, and crabs; by wing fanning in moths) or by changing the hair spacing (by passive splaying during the flick in crabs), the animals can alter the penetration of ambient fluid between their chemosensory hairs.

In order to assess how such changes in leakiness affect the molecule-capturing performance of olfactory antennae of various designs, we are using mathematical modeling to estimate the rates at which odorant molecules diffuse to the surfaces of chemosensory hairs under different flow conditions.

6. Molecule capture by chemosensory hairs on olfactory Antennae.

Molecule Capture by Stomatopod Antennules. In order to model the diffusion of odorant molecules to the surfaces of olfactory hairs, we must first determine the spatial distribution of odorant concentrations in the fluid arriving at the appendage bearing the sensory hairs. Although early analyses of animal navigation in odor plumes treated the plumes as evenly-diffusing clouds (e.g. Bossert and Wilson, 1968), more recent studies have revealed the heterogeneous distribution of odor concentrations in plumes in both water and air, and have suggested that animals might use this information in locating odor sources (e.g. Murlis and Jones, 1981; Kramer, 1986; 1992; Murlis, 1986; Murlis, et al., 1990; 1992; Mafra-Neto and Cardé, 1994; Weissburg and Zimmer-Faust, 1994; Willis, et al., 1994; Atema, 1995; Vickers and Baker, 1997; Baker, et al., 1998). Therefore, before calculating the transport of odorant molecules to stomatopod aesthetascs, we estimated realistic spatial distributions of odorant concentrations in the fluid encountered by stomatopod antennules. We used acoustic doppler velocimetry to

measure water velocity profiles and turbulence in stomatopod microhabitats in the field (Koehl and Cooper, unpublished data). Similar velocity profiles and fluctuations were then produced in a large laboratory flume (at the Environmental Fluid Mechanics Laboratory, Stanford) and planar laser induced fluorescence was used to study the spatial and temporal distribution of concentrations in dye plumes in the flume (Koehl, Koseff, Crimaldi, Cooper, McCay, Wiley, and Moore, unpublished data.) Our measurements revealed fine filaments of high concentration in the water arriving at animal antennules (Fig. 5).

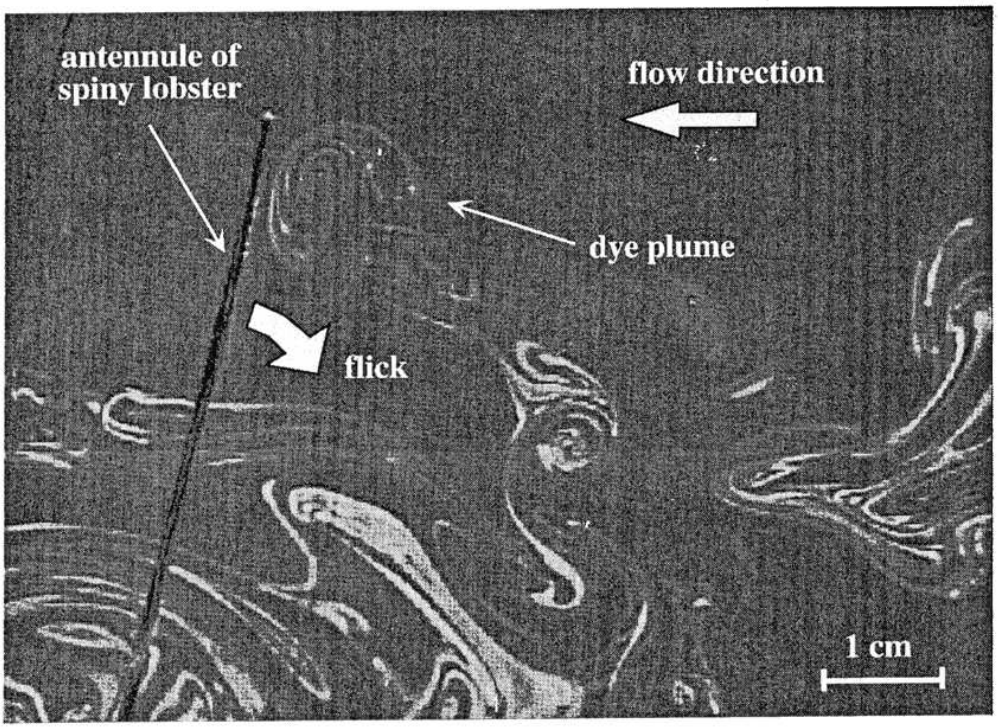

FIG. 5. *Frame of a video of a rhodamine dye plume in a flume (described in the text). A sheet of laser light illuminated the vertical plane in the flume in which the antennule of a spiny lobster was flicking (flick downstroke direction indicated by large arrow); that plane was parallel to the direction of water flow in the flume (indicated by large arrow). The antennule was ~1.5 m downstream from the "odor" source, a porous plate flush with the floor of the tank through which a solution of rhodamine "odor" was oozing. The lighter the water in the image, the higher the concentration of rhodamine dissolved in it. Note the fine filaments of high rhodamine concentration interspersed between thin layers of clean water. (Koehl, Koseff, Crimaldi, Cooper, McCay, Wiley, and Moore, unpublished data.)*

A two-dimensional advection-diffusion model was used to calculate the fate of odor filaments in water through which stomatopod antennules flick (Stacey, Mead, and Koehl, submitted). The velocity fields measured around dynamically-scaled physical models of stomatopod antennules (described above) were used to drive the advective component of the advection-diffusion equation. Odor filaments of various widths were carried in this

flow past the arrays of aesthetascs on an antennule; the concentration distribution in a filament at the start of each calculation was based on concentration measurements obtained by digitization of plume images similar to that shown in Fig. 5. Odorant molecules in a filament underwent molecular diffusion (diffusion coefficient of 10^{-5} cm^2/s) as the filament was carried in the flow through the aesthetasc array, and molecules encountering the surface of an aesthetasc were removed from the water (Fig. 6).

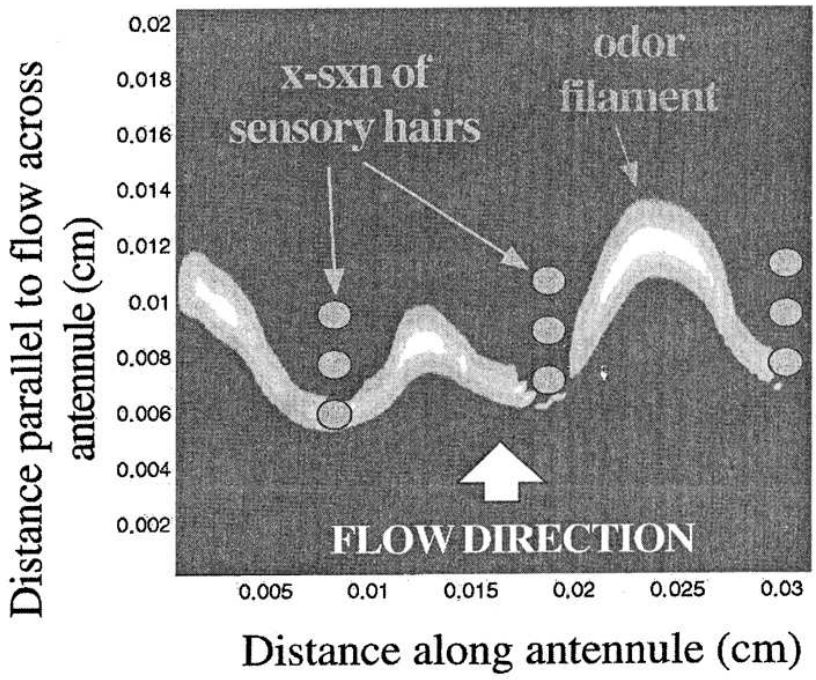

FIG. 6. *Diagram of one time step in the calculation of the molecular diffusion of an odor filament carried in water moving through the array of aesthetascs on the antennule of an adult stomatopod, Gonodactylus mutatus (Stacey, Mead, and Koehl, submitted). The long axis of the antennule is horizontal in the diagram, and the aesthetascs (which stick out of the page towards the reader) are shown in cross-section. The antennule is flicking downwards in the diagram, hence the flow direction relative to the aesthetascs is upwards in the diagram. The water velocity field around the aesthetascs was measured around a dynamically-scaled physical model (Mead and Koehl, in press). Odor filaments of various dimensions (digitized from images such as Fig. 5) were used in the calculations; a very thin filament is shown here. The lighter the water in the image, the higher the concentration of "odorant" dissolved in it. Any odorant molecule hitting the surface of an aesthetasc is removed from the water.*

Numerical simulations of such odor filament advection and diffusion enabled us to calculate the flux (molecules per time per area) of odorant molecules arriving at the surface of an aesthetasc as a function of time. One important aspect of the time course of odorant arrival at an aesthetasc is the peak flux attained. The importance of peak flux is indicated by experiments showing that chemosensory neurons in lobster antennules

produce more spikes when the peak concentration of odorant pulses delivered to them is higher (Gomez and Atema, 1996). The onset slope of a plot of odorant flux to the aesthetasc as a function of time is also likely to be important; Moore's (1994) mathematical model of adaptation and deadaptation in olfactory receptor neurons suggests that the rate at which odorant concentration increases can determine which chemosensory neurons fire. We used our advection-diffusion model to calculate peak odorant flux and onset slope for the aesthetascs on the antennules of adult stomatopods and on juveniles. We compared these parameters for an antennule encountering an odor filament during the rapid outward flick with those for an antennule encountering such a filament during the slower return stroke. For adults, the peak flux during an outstroke is 12 times greater than the peak flux during a return stroke, and the onset slope is 26 times greater during the outstroke than during the return. For juveniles, whose aesthetasc rows are spaced with a greater G/D than are those of adults, the differences between outstroke and return are even more striking: the peak flux is 26 times greater and the onset slope is 82 times greater during the rapid flick outstroke than during the slower return stroke.

Our advection-diffusion model of molecule transport to the surfaces of the aesthetascs of stomatopod antennules indicates that differences in water flow through aesthetasc arrays on these olfactory structures do indeed translate into differences in molecule capture by these antennules.

Molecule Capture by Moth Antennae. We have also used mathematical modeling to explore the effect on molecule capture by silkworm moth antennae of the increased antennal leakiness produced by wing fanning (Loudon and Koehl, in press). Because moths can sense pheromone molecules in very low concentrations in the air around them, we calculated the probabilities of encountering the chemosensory hairs (sensilla) for individual molecules undergoing random thermal motion in the air flowing through an antenna.

To calculate the probability of a pheromone molecule reaching the surface of a sensillum by diffusion once it has entered the gap between adjacent sensilla, we considered the one-dimensional random walk of odorant molecules perpendicular to the direction of air flow between the sensilla. The step length and frequency for the simulated random walks were determined, as explained in Berg (1993), from the diffusion coefficient (2.5×10^{-6} m^2/s in air at 20^oC) and molecular weight (238 g/mole) of bombykol, the primary molecular component of the sex pheromone of *B. mori* (Adam and Delbruck, 1968). We divided the gap between neighboring sensilla into 30 lanes and used our calculated velocity profiles between sensilla (described above) to determine the mean air velocity in each lane. Computer simulations were run of random walks by bombykol molecules entering the gap in each lane; molecules "walked" between lanes, so the velocity of the air carrying the molecule through the gap at each step depended upon the lane in which the molecule was located at the start of that step. The proportion

of simulated walks (500 walks were run per lane) that resulted in contact with either sensillum bounding a gap was used to estimate the probability of capture for molecules that entered the gap in each lane.

Our calculations showed that wing fanning can increase the rate of pheromone capture by the sensilla on *B. mori* antennae by two orders of magnitude over that of antennae on moths standing or walking in still air without fanning. Although a smaller proportion of the pheromone molecules in a parcel of air traveling through a gap between sensilla have time to diffuse to either of the sensilla when the air velocity is high than when it is low, faster air carries more molecules per time through the gap. Thus, as we found for stomatopod antennules, differences in air flow through arrays of sensory hairs on moth antennae do produce differences in molecule capture rates by these olfactory structures.

7. Conclusions. Appendages bearing arrays of hairs are important not only because they are found in so many different taxa, but also because they serve a variety of essential biological functions, such as feeding, locomotion, and molecule capture. Mathematical and physical modeling, done in conjunction with kinematic and morphometric studies of hairy legs on real animals, have revealed a number of patterns in how the flow through arrays of hairs depends on their structure and behavior. Rows of hairs operating at Re > 1 function like leaky sieves (unless the hairs are very close together), whereas those operating at Re $\leq 10^{-2}$ function like paddles, with very little fluid moving between adjacent hairs. The Re range in which the transition in leakiness occurs depends on the geometry of the appendage: the wider the gap (G) between neighboring hairs relative to hair diameter (D), the lower the Re at which this transition between paddle-like and sieve-like function occurs. At Re's of order 1, the leakiness of arrays of closely-spaced hairs (i.e. arrays with low G/D) is very sensitive to hair spacing and to flow velocity. The chemosensory hairs on a variety of olfactory antennae operate in a range of Re's and hair spacings in which changes in velocity and changes in hair spacing can have profound effects on the flow near the hairs, and thus on their performance in capturing molecules from the surrounding fluid.

Acknowledgements. This research was supported by grants from the Office of Naval Research, U.S.A. (#N00014-96-1-0594 and #N00014-98-1-0775, to M. Koehl) and the Hasselblad Foundation (to M. Koehl and C. Loudon), by an Augmentation Award for Science and Engineering Research Training, Department of Defense, U.S.A. (#N00014-97-1-0726, to M. Koehl), and by a fellowship from the John D. and Catherine T. MacArthur Foundation (to M. Koehl). I am grateful to D. Abdullah, B. Best, A. Cheer, T. Cooper, J. Crimaldi, J. Goldman, W. Hu, J. Koseff, C. Loudon, M. Martinez, K. Mead, P. Moore, M. Stacey, and M. Wiley for collaborating on various aspects of the work cited here; and to L. Castillo, L. Gorsky, and U. Lee for help with digitizing.

REFERENCES

ACHE, B.W. (1982). Chemoreception and thermoreception. pp. 369–393 In H.L. Atwood and D.C. Standeman, eds. *The Biology of the Crustacea*, Vol. **3.**, New York, Academic Press.

ACHE, B.W. (1988). Integration of chemosensory information in aquatic invertebrates. In J. Atema and et. al., eds. *Sensory Biology of Aquatic Animals.* New York, Springer-Verlag.

ADAM, G. AND M. DELBRUK (1968). Reduction in dimensionality in biological diffusion processes. pp. 198–215 In *Structural Chemistry and Molecular Biology.* A. Rich and N. Davidson, eds., W.H. Freeman and Co., San Francisco.

ATEMA, J. (1977). Functional separation of smell and taste in fish and crustacea. pp. 165–174 In J. LeMagnen and L. MacLeod, eds. *Olfaction and Taste IV.* London, Information Retrieval.

ATEMA, J. (1985). Chemoreception in the sea: Adaptations of chemoreceptors and behavior to aquatic stimulus conditions. *Soc. Exp. Biol. Symp.* **39**:3887–3423.

ATEMA, J. (1995). Chemical signals in the marine environment: Dispersal, detection and temporal analysis. pp. 147–159 In *Chemical Ecology: The Chemistry of Biotic Interaction.* Academy Press, Washington, D.C.

ATEMA, J. AND R. VOIGT (1995). Behavior and Sensory Biology. pp. 313–348 In J.R. Factor, eds. *Biology of the Lobster Homarus americanus.* San Diego, CA, Academic Press.

BAKER, T.C., H.Y. FADAMIRO, AND A.A. COSSE (1998). Moth uses fine tuning for odour resolution. *Nature* **393**:530.

BERG, H.C. AND E.M. PURCELL (1977). Physics of Chemoreception. *Biophys. J.* **20**:193–217.

BOECKH, J., K.E. KAISSLING, AND D. SCHNEIDER (1965). Insect olfactory receptors. *Cold Spring Harbor Symp. Quant. Biol.* **30**:263–280.

BOSSERT, W.H. AND E.O. WILSON (1963). The analysis of olfactory communication among animals. *J. Theor. Biol.* **5**:443–469.

CARD, R.T. (1984). Chemo-orientation in flying insects. pp. 109–134. In W.J. Bell and R.T. Cardé, eds. *Chemical Ecology of Insects.* Elsevier Press, Amsterdam.

CHEER, A.Y.L. AND M.A.R. KOEHL (1987a) Paddles and rakes: Fluid flow through bristled appendages of small organisms. *J. Theor. Biol.* **129**:185–199.

CHEER, A.Y.L. AND M.A.R. KOEHL (1987b). Fluid flow through filtering appendages of insects. *IMA J. Math. Appl. Med. Biol.* **4**:185–199.

DAVIES, C.N. (1973). *Air Filtration.* Academic Press, New York.

DESIMONE, J.A. (1981). Physicochemical principles in taste and olfaction, pp. 213–229. In *Taste and Olfaction.* Academic Press, New York.

FUCHS, N.A. (1964). *The Mechanics of Aerosols.* Oxford University Press, Oxford.

FUTRELLE, R.P. (1984). How molecules get to their detectors: The physics of diffusion of insect pheromones. *Trans. Neorosci.* April, 116–120.

GETCHELL, T.V. AND M.L. GETCHELL (1977). Early events in vertebrate olfaction. *Chem. Senses* **2**:313–326.

GLEESON, R.A. (1982). Morphological and behavioral identification of the sensory structures mediating pheromone reception in the blue crab, *Callinectes sapidus. Biol. Bull.* **163**:162–171.

GLEESON, R.A., W.E.S. CARR AND H.G. TRAPIDO-ROSENTHAL (1993). Morphological characteristics facilitating stimulus access and removal in the olfactory organ of the spiny lobster, *Panulirus argus*: Insight from the design. *Chemical Senses.* **18**:67–75.

GNATZY, W., W. MOHREN, AND R.A. STEINBRECHT (1984). Pheromone receptors in Bombyx mori and *Antheraea pernyi.* II. Morphometric analysis. *Cell Tiss. Res.* **235**:35–42.

GOLDMAN, J.A. AND M.A.R. KOEHL. Fluid dynamic design of lobster olfactory organs: High-speed kinematic analysis of antennule flicking in *Panulirus argus: Chemical Senses* (submitted).

GOMEZ, G. AND J. ATEMA (1996). Temporal resolution in olfaction: Stimulus integration time of lobster chemoreceptor cells. *J. Exp. Biol.* **199**:1771–1779.

GRUNERT, U. AND B.W. ACHE (1988). Ultrastructure of the aesthetasc (olfactory) sensilla of the spiny lobster *Panulirus argus*. *Cell Tissue Res.* **251**:95–103.

HALLBERG, E., K.U.I. JOHANSSON AND R. ELOFSSON (1992). The aesthetasc concept: Structural variations of putative olfactory receptor cell complexes in crustaceans. *Microsc. Res. Techn.* **22**:336–350.

HANSEN, B. AND P. TISELIUS (1992). Flow through the feeding structures of suspension feeding zooplankton: A physical model approach. *J. Plankton Res.* **14**:821–834.

HEIMANN, P. (1984). Fine structure and molting of the aesthetasc sense organs on the antennules of the isopod, *Asellus aquaticus* (Crustacea). Cell Tissue Res. **235**:117–128.

KOEHL, M.A.R. (1993). Hairy little legs: Feeding, smelling, and swimming at low Reynolds numbers. *Contemp. Math.* **141**:33–64.

KOEHL, M.A.R. (1995). Fluid flow through hair-bearing appendages: Feeding, smelling, and swimming at low and intermediate Reynolds number. In C.P. Ellington, T.J. Pedley, eds., *Biological Fluid Dynamics, Soc. Exp. Biol. Symp.* **49**:157–182.

KOEHL, M.A.R. (1996). Small-Scale fluid dynamics of olfactory antennae. *Mar. Fresh. Behav. Physiol.* **27**:127–141.

KOEHL, M.A.R. (1998). Small-Scale hydrodynamics of feeding appendages of marine animals. *Oceanogr.* 11:10–12.

KOEHL, M.A.R. AND J.R. STRICKLER (1981). Copepod feeding currents: Food capture at low Reynolds number. *Limnol. Oceanogr.* **26**:1062–1073.

KOO, J.-K. AND D.F. JAMES (1973). Fluid flow around and through a screen. *J. Fluid Mech.* **60**:513–538.

KRAMER, E. (1986). Turbulent diffusion and pheromone-triggered anemotaxis, pp. 59–67. In T.L. Payne, M.C. Birch and C.E.J. Kennedy, eds. *Mechanisms in Insect Olfaction.* Oxford: Clarendon Press.

KRAMER, E. (1992). Attractivity of pheromone surpassed by time-patterned application of two nonpheromone compounds. *J. Insect Behav.* **5**:83–97.

LABARBERA, M. (1984). Feeding currents and particle capture mechanisms in suspension feeding animals. *Am. Zool.* **24**:71–84.

LAVERACK, M. S. (1988). The diversity of chemoreceptors, pp. 287–317 In Atema, J. [ed.], *Sensory Biology of Aquatic Animals.* Springer-Verlag, New York.

LAWS, E.M. AND J.L. LIVESEY (1978). Flow through screens. *Ann. Rev. Fluid Mech.* **10**:247–266.

LEONARD, A.B.P. (1992). *The Biomechanics, Autecology and Behavior of Suspension-Feeding in Crinoid Echinoderms.* Ph.D. Dissertation, University of California, San Diego.

LOUDON, C. (1990). Empirical test of filtering theory: Particle capture by rectangular-mesh nets. *Limnol. Oceanogr.* **35**:143–148.

LOUDON, C., B.A. BEST, AND M.A.R. KOEHL (1994). When does motion relative to neighboring surfaces alter the flow through an array of hairs? *J. Exp. Biol.* **193**:233–254.

LOUDON, C. AND M.A.R. KOEHL. Sniffing by a silkworm moth: Wing fanning enhances air penetration through and pheromone interception by antennae. *J. Exp. Biol.* (in press).

MAFRA-NETO, A. AND R.T. CARD (1994). Fine-scale structure of pheromone plumes modulates upwind orientation of flying moths. *Nature* **369**:142–144.

MANKIN, R.W. AND M.S. MAYER (1984). The insect antenna is not a molecular sieve. *Experientia* **40**:1251–1252.

MARSCALL, H.-P. AND B.W. ACHE (1989). Response dynamics of lobster olfactory neurons during simulated natural sampling. *Chem. Senses* **14**:725.

MEAD, K.S., M.A.R. KOEHL, AND M.J. O'DONNELL. (1999). Stomatopod sniffing: The scaling of chemosensory sensillae and flicking behavior with body size. *J. Exp. Mar. Biol. Ecol.* **241**:235–261.

MEAD, K.S. AND M.A.R. KOEHL. Stomatopod antennule design: The asymmetry, sampling efficiency, and ontogeny of olfactory flicking. *J. Exp. Biol.* (in press).

MICHEL, W.C., T.S. MCKLINTOCK, AND B.W. ACHE (1991). Inhibition of lobster olfactory receptor cells by an odor-activated potassium conductance. *J. Neurophysiology* **65**:446–453.

MOORE, P.A. (1994). A model of the role of adaptation and disadaptation in olfactory receptor neurons: implications for the coding of temporal and intensity patterns in odor signals. *Chemical Senses.* **19**:71–86.

MOORE, P.A., J. ATEMA AND G.A. GERHARDT (1991). Fluid dynamics and microscale chemical movement in the chemosensory appendages of the lobster, *Homarus americanus. Chemical Senses* **16**:663–674.

MOORE, P.A., G.A. GERHARDT, AND J. ATEMA (1989). High resolution spatio-temporal analysis of aquatic chemical signals using microchemical electrodes. *Chemical Senses* **14**:829–840.

MURLIS, J. (1986). The structure of odour plumes, pp. 27–38. In T.L. Payne, ed. *Mechanisms of Insect Olfaction*, Clarendon Press, NJ.

MURLIS, J., J.S. ELKINTON, AND R.T. CARD (1992). Odor plumes and how insects use them. *Ann. Rev. Entomol.* **37**:505–532.

MURLIS, J. AND C.D. JONES (1981). Fine-scale structure of odour plumes in relation to insect orientation to distant pheromone and other attractant sources. *Physiol. Entomol.* **6**:71–86.

MURLIS, J., M.A. WILLIS AND R.T. CARDÉ (1990). Odour signals: patterns in time and space, pp. 6–17 In K. Doving, ed. *Proceedings of the X International Symposium on Olfaction and Taste, Oslo.*

MURRAY, J.D. (1977). Reduction of dimensionability in diffusion processes: Antenna receptors of moths, pp. 83–127 In *Lectures on Nonlinear-Differential-Equation Models in Biology*, Oxford University Press, Oxford.

NACHBAR, R.B. AND T.H. MORTON (1981). A gas chromatograph (GPLC) model for the sense of smell: Variations of olfactory sensitivity with conditions of stimulation. *J. Theor. Biol.* **84**:387–407.

POPHOF, B. (1997). Olfactory responses recorded from sensilla coeloconica of the silkworm *Bombyx mori. Physiol. Entomol.* **22**:239–248.

RUBENSTEIN, D.I. AND M.A.R. KOEHL (1977). The mechanisms of filter feeding: Some theoretical considerations. *Amer. Natur.* **26**:981–994.

SCHMIDT, B.C. AND B.W. ACHE (1979). Olfaction: Responses of a decapod crustacean are enhanced by flicking. *Science* **205**:204–206.

SHIMETA, J. AND P.A. JUMARS, (1991). Physical mechanisms and rates of particle capture by suspension-feeders. *Oceanogr. Mar. Biol. Annu. Rev.* **29**:191–257.

SILVESTER, N.R. (1983). Some hydrodynamic aspects of filter feeding with rectangular-mesh nets. *J. Theor. Biol.* **103**:265–286.

SNOW, P.J. (1973). The antennular activities of the hermit crab, *Pagarus alaskensis* (Benedict). *J. Exp. Biol.* **58**:745–765.

SPEILMAN, L.A. AND S.L. GOREN (1968). Model for predicting pressure drop and filtration efficiency in fibrous media. *Environ. Sci. Technol.* **2**:279–287.

STACEY, M., K.S. MEAD, AND M.A.R. KOEHL. Molecule capture by olfactory antennules: Mantis shrimp. *J. Math. Biol.* (submitted).

STEINBRECHT, R.A. (1992). Experimental morphology of insect olfaction: tracer studies, x-ray microanalysis, autoradiography, and immunochemistry with silkmoth antennae. *Microscopy Res. and Tech.* **22**:336–350.

TAMADA, K. AND H. FUJIKAWA (1957). The steady two-dimensional flow of viscous fluid at low Reynolds numbers passing through an infinite row of equal parallel circular cylinders. *Quart. J. Mech. Appl. Math.* **10**:425–432.

TAYLOR, G.I. AND G.K. BATCHELOR (1949). The effects of wire gauze on small disturbances in uniform stream. *Quart. J. Mech. Appl. Math.* **2**:1–29.

VICKERS, N.J. AND T.C. BAKER (1997). Flight of *Heliothis virescens* males in the field in response to sex pheromone. *Physiol. Entomol.* **22**:277–285.

VOGEL, S. (1983). How much air passes through a silkmoth's antenna? *J. Insect Physiol.* **29**:597–602.

WEISSBURG, M.J. AND R.K. ZIMMER-FAUST (1994). Odor plumes and how blue crabs use them in finding prey. *J. Exp. Biol.* **197**:349–375.

WILLIS, M.A., C.T. DAVID, J. MURLIS AND R.T. CARDÉ (1994). Effects of pheromone plume structure and visual stimuli on the pheromone-modulated upwind flight of male gypsy moths (Lumantria dispar) in a forest (Lepidoptera, Lymantriidae). *J. Insect Behav.* **7**:385–409.

ZACHARUK, R.Y. (1985). Antennae and sensilla, pp. 1–69. In G.A. Kerkut and L.I. Gilbert, eds. *Comprehensive Insect Physiology, Biochemistry and Pharmacology,* New York, Pergamon Press.

ZIMMER-FAUST, R.K. (1989). The relationship between chemoreception and foraging behavior in crustaceans. *Limnol. Oceanogr.* **34**:1367–1374.